RFI CANCELLATION IN VDSL SYSTEMS USING A NOVEL COMPLEX ALLPASS-BASED IIR ADAPTIVE NOTCH FILTER

F. H. Gregorio ◇ † [1], *J. E. Cousseau* * [2], *and T. I. Laakso* † [1]

[1]Helsinki University of Technology, Signal Processing Laboratory, P.O. Box 3000, FIN-02015 HUT, Finland.
[2] Universidad Nacional del Sur, Dept. of Electrical and Computer Eng., Av. Alem 1253, 8000, Bahía Blanca, Argentina
fernando.gregorio@hut.fi

ABSTRACT

A complex-allpass-based multiple notch IIR filter is proposed to suppress Radio Frequency Interference (RFI) that affect VDSL systems. A notch filter realization based on complex allpass cascaded second-order sections is presented and evaluated in this paper. Two different algorithms, using the Recursive Prediction Error (RPE) method and an alternative (similar to the Steiglitz-McBride) method, are proposed to update the adaptive notch filter coefficients. Simple stochastic gradient algorithms can be obtained using allpass cascaded second-order sections whose regressors are formed by orthogonal functions which is not the case for the conventional complex cascade realization. Comparisons with other multiple-notch realizations evaluating convergence rate and residual interference levels are included. The novel structure using the RPE method reaches the lowest residual interference level with the fastest convergence rate. Furthermore using the novel techniques stability check is not needed, which reduces their implementation complexity.

1. INTRODUCTION

Digital Subscriber Line (DSL) transmission is one of the fastest growing telecommunication technologies. Since twisted pair wires in the telephone network are unshielded and many wires are tightly bundled, there are a number of interferences that must be considered. For the particular cases of VDSL, Single Carrier and Multicarrier implementations, crosstalk, radio frequency interference (RFI) and impulsive noise (IN) are the main disturbances to be considered [1]. Radio-frequency interference (RFI) caused by broadcast AM radio transmitters and radio amateurs is considered to be one of the most challenging problems. Especially the interference from radio amateurs (HAM interference) is difficult to handle. It is non-stationary, as the transmission is intermittent and bursty, and exhibits potentially high power levels when transmitters are close to the wiring. RFI effects can be reduced using specific transmission masks. However, HAM interferences can change their frequency band, often imposing the additional constraint that any RF canceler needs to be adaptive.

An adaptive RFI canceler should converge fast to the incident frequency and be able to track the variation of the RFI frequency. On the other hand, suppression level of 40 dB must be obtained. IIR filter realizations, i.e. IIR adaptive notch filters (ANF), are used instead of FIR structures because FIR structures require large filter order to obtain this level of suppression with sharp cutoff characteristics [2] [3].

An allpass-based IIR multiple Complex Adaptive Notch Filter (CANF) is presented in this work, with two different algorithms, associated to the Recursive Prediction Error (RPE) method (A1-CANF) and an alternative method (A2-CANF) which is similar to the Steiglitz-McBride method, based on different minimization criteria. A real-coefficient version of this realization was proposed in [4]. Both algorithms are evaluated in an RFI interference cancellation application.

The motivations to introduce the factorized all-pass IIR notch model for multiple complex signals is the direct availability in the realization of an orthogonal set of functions useful when measurement noise is of concern.

In order to demonstrate their advantage in terms of convergence speed, their performance are compared with the conventional cascaded complex implementation (C-CANF) [5] and the complex notch filter with direct-form realization (D-CANF) [6].

The paper is organized as follows. RFI signals and the conventional complex cascaded IIR multiple notch filter are reviewed in Section 2. The complex allpass-based multiple notch filter is presented in Section 3. In addition in this section two related updating algorithms proposed for the new realization. Simulation results in the RFI cancellation application comparing the new algorithms with other realizations are presented and discussed in Section 4. Conclusions are drawn in the last section.

2. RFI AND IIR COMPLEX ANF

This work focuses on the detection and cancellation of RFI interferences. For VDSL systems, the usable bandwidth is extended between 1.1 to 30 MHz depending on the loop length. There are many amplitude modulated (AM) radio stations in the frequency band of 0.55 to 1.7 MHz, and SW radio stations located in several bands between 1.7 and 30 MHz. There are also amateur short wave frequency bands distributed in the same range. RFI signal can reach power density levels with values up to -40 dBm/Hz in HAM bands as is recognized in ANSI and ETSI standards [7].

A RFI signal can be represented in the time domain as

$$u(k) = \sum_{i=1}^{M} A_i e^{jw_i} + n(k) \qquad (1)$$

where k is the time index, w_i and A_i are the frequency and the amplitude of interference i, respectively, M is the number of interference signals and $n(k)$ is a complex Gaussian random noise process modeling the VDSL signal. The VDSL signal

◇ Supported by the Programme ALβAN, European Union Programme of High Level Scholarships for Latin America. Identification Number:**E03D19254AR**

* This work was partially supported by Agencia Nacional de Promocion Cientifica y Tecnologica, Argentina, Project # PICT 07101.

† Fernando Gregorio and Timo Laakso are with the Smart and Novel Radios Research Group (SMARAD) Center of Excellence.

can be modeled with a flat power spectral density of -60 dBm/Hz [8].

Cascade Complex ANF (C-CANF)

Conventional cascade complex multiple notch filter (C-CANF) can be described by the transfer function

$$H_c(z) = \prod_{i=1}^{M} H_i(z) = \prod_{i=1}^{M} \frac{1 - e^{j\omega_i} z^{-1}}{1 - \rho_i e^{j\omega_i} z^{-1}} \tag{2}$$

where ω_i is the notch angular frequency and ρ_i is the filter pole radius that determines the notch bandwidth.

The input signal $u(k)$ is composed of a narrowband signal (RFI interference) and a wideband signal (VDSL). The output of the notch filter contains only the broadband signal when the filter coefficients are adjusted. The output of the cascaded notch filter is given by $y_M(k) = H_c(q^{-1})u(k)$. The coefficients are chosen to minimize the notch filter output power, i.e., $E[|y_M(k)|^2]$. The updating algorithm proposed in [5] takes the form

$$\omega_i(k+1) = \omega_i(k) - \frac{\mu}{r_{rpe}(k)} \mathrm{Re}[y_M(k)\varphi_i^*(k)] \tag{3}$$

$$r_{rpe}(k+1) = (1-\lambda) r_{rpe}(k) + \lambda(\varphi_i(k)\varphi_i^*(k)) \tag{4}$$

where

$$\varphi_i(k) = -\frac{j e^{j\omega_i} q^{-1}}{1 - \rho_i e^{j\omega_i} q^{-1}} \left(\prod_{n=1, n\neq i}^{M} H_n(q^{-1}) \right) u(k) \tag{5}$$

Direct realization Complex ANF (D-CANF)

An illustrative use of this implementation can be found in [6]. The notch filter is defined as

$$H_D(z) = \frac{1 + \sum_{i=1}^{M} a_i^* z^{-i}}{1 + \sum_{i=1}^{M} \rho_i a_i^* z^{-i}} \tag{6}$$

where ρ is the filter pole radius and a_i is the parameter of the filter, and M is the number of notches. The order of the filter is related with the number of tones to be cancel. The parameter vector is $\theta = [a_1, a_2 \ldots a_M]^T$ which will be adjusted by minimizing the output signal power. In [6], a Gauss-Newton algorithm is implemented with an exponential profile variation for the filter pole radius ρ. Stability check must be included, which increases the algorithm complexity.

3. NOVEL ALLPASS-BASED CANF (A-CANF)

The model for the proposed allpass-based multiple complex adaptive notch filter (A-CANF) can be described by

$$H(z) = \frac{1}{2}(1 + \prod_{i=1}^{M} V_i(z)) \tag{7}$$

where $V_i(z) = \frac{\rho_i - e^{j\omega_i} z^{-1}}{1 - \rho_i e^{j\omega_i} z^{-1}}$ and ρ_i is the corresponding pole radius to ω_i ($0 < \rho < 1$). In order to facilitate the analysis and presentation, the following relationships will be useful

$$\begin{aligned} V_i(e^{j\omega}) &= \cos(\phi_i(\omega)) + j\sin(\phi_i(\omega)) = exp[j\phi_i(\omega)] \\ &= \frac{1}{|D_i(e^{j\omega})|^2} \left[\left(2\rho_i - (1+\rho_i^2)\cos(\omega_i - \omega)\right) \right. \\ &\quad \left. - j\left((1-\rho_i^2)\sin(\omega_i - \omega)\right) \right] \end{aligned} \tag{8}$$

where $D_i(e^{j\omega}) = 1 - \rho_i e^{j\omega_i} e^{-j\omega}$ and $\phi_i(\omega)$ is the phase of the corresponding allpass section i. Note that when $\rho_i \to 1$, $\phi_i(\omega) \to \pi$. (7) does not describe in general the same transfer function as (2). However, it is easy to verify using (8) that a very close behavior can be obtained with both models for $\rho_i \to 1$.

The main advantage of the new complex multiple-notch model is related to its application in the context of adaptive filtering in general, and narrowband signal (for example, RFI) cancellation. As will be discussed in the following subsections, simple stochastic gradient algorithms can be obtained with this model whose regressors are formed by orthogonal functions. Note that this is not the case for the complex cascade realization. This property leads in general to estimates that are less sensitive to the signal-to-interference ratio (SIR) level. The basic orthogonal signals of interest are the following

$$F_i(z) = \frac{z^{-1}}{D_i(z)} \prod_{k=1, k\neq i}^{M} V_i(z) \tag{9}$$

In order to complete the model definition of (7), an exponential profile variation is considered for each allpass section pole radius ρ_i, given by

$$\rho_i(k+1) = r_i \rho_i(k) + (1 - r_i)\rho_i^{\infty} \tag{10}$$

where r_i defines the exponential decay time constant and ρ_i^{∞} is the asymptotic value of ρ_i.

Recursive Prediction Error Algorithm (A1-CANF): Looking for the minimization of the output signal power, based on the model (7), the conventional recursive prediction error method can be used [9]. This method leads to the following normalized stochastic gradient updating algorithm

$$\begin{aligned} w_{rpe_i}(k+1) &= w_{rpe_i}(k) - \frac{\mu}{r_{rpe}(k)} \mathrm{Re}[y_M(k)\psi_i^*(k)] \\ r_{rpe}(k+1) &= (1-\lambda) r_{rpe}(k) + \lambda(\psi_i(k)\psi_i^*(k)) \end{aligned} \tag{11}$$

where

$$\psi_i(k) = -\frac{j e^{j\omega_i} q^{-1}}{D_i(q^{-1})} \left(\prod_{n=1, n\neq i}^{M} V_n(q^{-1}) \right) u(k)$$

λ is the forgetting factor and μ is the step size. A block diagram of the complex allpass-based multiple notch realization is illustrated in Figure 1.

Local convergence of this algorithm can be easily verified using standard linearized Liapunov arguments. For $\rho_i \to 1$ unbiased estimates can be obtained. More interesting is the fact that the regressor components are formed by orthogonal functions. Following the ODE analysis of the stationary points related to (11) [2], and assuming the disturbance $n(k)$ is white noise, then these stationary points can be shown to be free from any noise-induced component.

An alternative Algorithm (A2-CANF): An alternative updating algorithm can be obtained following an approach similar to [10] [2] [4]. Based in the model (7), we consider the minimization of the variance of the following signal

$$\overline{e}_M(k+1) = \frac{1}{2} \frac{\prod_{i=1}^{M} D_i^{(k+1)}(q^{-1}) + \prod_{i=1}^{M} \overline{D}_i^{(k+1)}(q^{-1})}{\prod_{i=1}^{M} D_i^{(k)}(q^{-1})} u(k) \tag{12}$$

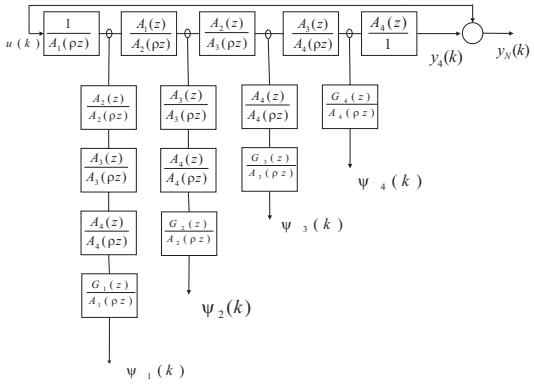

Figure 1: Block diagram of A1-CANF implementation.

where $D_i^{(k)}(z) = 1 - \rho e^{j\omega_i(k)} z^{-1}$ and $\overline{D}_i^{(k)}(z) = [D_i^{(k)}(1/z^*)]^*$. At time $k+1$, assuming $D_i^{(k)}(z)$ known, this signal is linear in the coefficients. In an on-line implementation we can consider $\overline{e}_M(k) \cong y_M(k)$. By differentiating (12) with respect to the frequencies ω_i, the regressor is obtained in the following form:

$$\psi_i(k) = -\frac{je^{j\omega_i} q^{-1}}{D_i(q^{-1})} \left(\prod_{n=1, n\neq i}^{M} (1 + V_n(q^{-1}) \right) u(k)$$

and the updating equations for a normalized stochastic gradient algorithm are described by (A2-CANF)

$$\omega_{sm_i}(k+1) = \omega_{sm_i}(k) - \frac{\mu}{r_{sm}(k)} \mathrm{Re}[y_M(k)\psi_i^*(k)] \qquad (13)$$
$$r_{sm}(k+1) = (1-\lambda) r_{sm}(k) + \lambda(\psi_i(k)\psi_i^*(k))$$

where λ is the forgetting factor and μ is the step size.

Local convergence of this algorithm can be verified in a form similar to that in [4]. Following that approach, unbiased estimates can be obtained for $\rho_i \to 1$. Due to the regressor definition (which includes the orthogonal functions of (9)), and assuming a white noise disturbance, the ODE analysis of (13) has no noise-induced component.

A detailed evaluation of these properties and other characteristics of the proposed algorithms are presented in the following section.

4. SIMULATIONS AND COMPARISONS

The performance of the four algorithms, is evaluated in this section to suppress RFI interference in a VDSL system using single-carrier modulation. The VDSL signal is modeled as white noise with PSD equal to -60 dBm/Hz in the normalized bandwidth. RFI consists of up to 4 complex sinusoids with higher amplitudes than the VDSL signal and frequencies varying inside the complete VDSL bandwidth.

Different exponential profiles are defined for each filter section, and for each realization. The initial values are $\rho_j = 0.9$ with different exponential time decay constants, $r_0 = [0.75, 0.6, 0.65, 0.55]$ for each section, asymptotic value $\rho_0^\infty = 0.975$, forgetting factor $\lambda = 0.01$ and $\mu = 0.01$.

Figure 2 depicts the coefficient evolution that give the frequency notch of the filter considering 4 RFI signals with normalized frequencies given by $\omega = [0.2, 0.4, 0.6, 0.8]$ and $SIR = 20$ dB. Direct implementation method is not shown in this figure due to the coefficient evolution don't express the frequency notch in direct way.

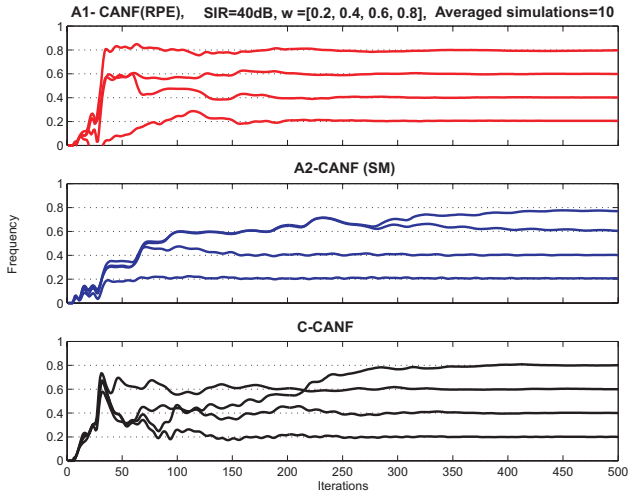

Figure 2: Learning curve for A1-CANF, A2-CANF and C-CANF with high SIR=40dB

Implementation	No. iterations			MSE [dB]		
	C1	C2	C3	C1	C2	C3
A1-CANF	681	400	820	-33.59	-16.95	-14.5
A2-CANF	1281	602	1310	-33.92	-17.02	-13.8
C-CANF	714	415	850	-32.98	-16.21	-13.54
D-CANF	10500	770	11600	-33.1	-16.8	-13.45

Table 1: Simulation results - Number of iterations and minimum MSE

Mean Squared Error (MSE) evolution for the different algorithms are presented in Figure 3. In all simulations an excellent cancellation level is obtained. However, A1-CANF and A2-CANF implementations have reduced complexity compared with the others because the stability check is not necessary.

When only 2 RFI signals are present , the convergence speed of all algorithms is similar, with the best results for A1-CANF (RPE) implementation. All algorithms reach similar levels of residual interference.

In low SIR levels -2 dB, the best results were obtained using A2-CANF implementation with the fastest convergence speed and lowest residual error. Figure 4 shows the coefficient evolution for A2-CANF (SM) and C-CANF.

Table 1 summarizes the simulation results for the three cases: **C1**: SIR=40dB, 4 RFI signals, **C2**: SIR=20dB, 2 RFI signals and **C3**: SIR=20dB, 4 RFI signals. The number of iterations in which the algorithm converges (an average value of a window of twenty samples is considered) and the minimum MSE that is reached (after convergence) are included in this table. As illustrated using these simulations, and after using other contexts of interference cancellation, we can conclude that CANF versions reach faster convergence speed than direct implementation when 4 RFI interferences are included. A1-CANF version achieves the best performance in high SIR levels with a fast convergence speed and a low residual interference level. In a low SIR case, A2-CANF implementation had the fastest convergence rate with the lowest bias. Figure 4 shows the learning curve for A2-CANF and C-CANF algorithms.

The tracking performance is analyzed varying $\omega_1 = .2$ between 0.1 and 0.3 from samples 2000 to 3000 and 4000 to 4500 and $\omega_1 = 0.8$ varying to 0.9 from samples 2500 to 2900 with SIR=20dB as illustrated by Figure 5. The best re-

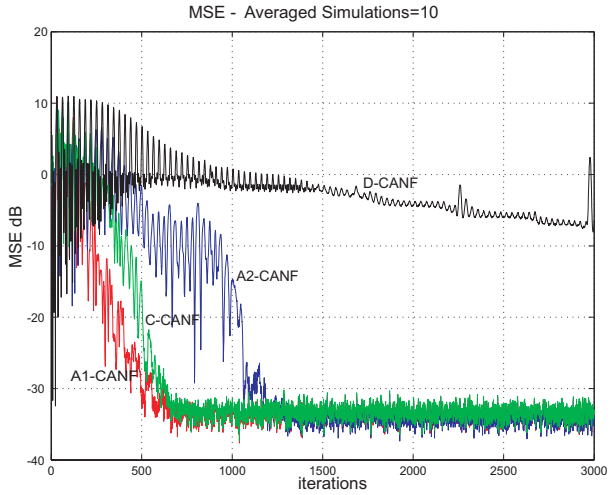

Figure 3: MSE Comparison for C-CANF, A1-CANF, A2-CANF and CDANF implementation. 4 RFI signals SIR=40dB (Averaged simulations=10)

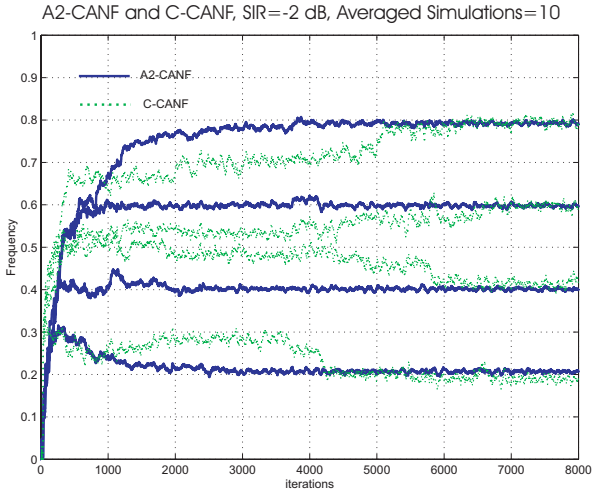

Figure 4: Learning curve for A2-CANF and C-CANF with low SIR=-2dB , $\omega = [0.2, 0.4, 0.6, 0.8]$

sults are obtained using A2-CANF method. A2-CANF (SM) follows the frequency change with a fast response without affecting the other frequency notches. The other methods had a good tracking response but the frequency estimation of the other notches is affected by the frequency variations of ω_1.

5. CONCLUSIONS

A new family of allpass-based complex IIR ANF was presented in this paper. Their performance was evaluated in RFI canceling application compared against the conventional complex cascaded and direct complex notch filters. The best results were reached using A1-CANF that showed the fastest convergence speed and the lowest residual interference level in high SIR levels. Steiglitz-McBride implementation (A2-CANF) had an excellent performance with low SIR levels.

Using the novel implementation simple stochastic gradient algorithms can be obtained using allpass cascaded second-order sections whose regressors are formed by orthogonal functions. Moreover, cascaded allpass second-

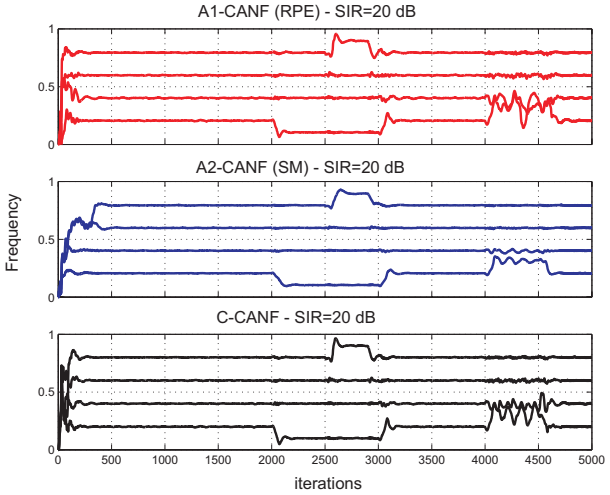

Figure 5: Learning curve for the tracking application where some RFI frequencies have step changes at 2000, 3000, 4000 and 4500 samples

order sections are implemented with low complexity because stability check is not needed.

These characteristics allow us to present the novel CANF algorithm as a good candidate for RFI canceling and other applications where tracking capability and low residual error are required. Other contexts like tracking, adaptive line enhancing (ALE) or tone detection in low-signal to noise ratio environments can be considered. Some of these subjects are currently under investigation.

REFERENCES

[1] T. Starr, J. Cioffi, and P. Silverman, *Understanding Digital Subscriber Lines*, Prentice Hall, 1999.

[2] P. Regalia, *Adaptive IIR Filtering in Signal Processing and Control*, Marcel Dekker, 1995.

[3] P. Stoica and A. Nehorai, "Performance analysis of an adaptive notch filter with constrained poles and zeros," *IEEE Trans. Acoust., Speech Signal Proc.*, vol. 36, no. 2, Feb. 1988.

[4] J. Cousseau, P. Doñate, and Y. Liu, "Factorized allpass-based IIR adaptive notch filters," in *IEEE Int. Conf. Acout. Speech, Signal Proc.*, May 2004, vol. 2, pp. 661–664.

[5] S. Nishimura and H.-Y. Jiang, "Gradient based complex adaptive IIR Notch Filters for Frequency Estimation," in *Proc. of IEEE Asia Pacific Conference on Circuits and Systems*, Nov. 1996, vol. 1, pp. 235–238.

[6] S.-C. Pei and C.-C. Tseng, "Complex Adaptive IIR Notch Filter Algorithm and its applications," *IEEE Trans. on Circuit and Systems - II*, vol. 41, no. 2, pp. 158–163, Feb. 1994.

[7] W. Chen, *DSL: Simulation Techniques and Standards Development for Digital Subscriber Lines*, Macmillan, 1998.

[8] Y. Liu, P. Diniz, and T. Laakso, "Adaptive Steiglitz-McBride notch filter design for radio interference suppression in VDSL systems," in *Proc. IEEE GLOBECOM 2001*, Nov. 2001, vol. 1, pp. 359–363.

[9] A. Nehorai, "A minimal parameter adaptive notch filter with constrained poles and zeros," *IEEE Trans. Acoust., Speech Signal Proc.*, vol. 43, no. 2, pp. 983–996, 1985.

[10] J. Travassos-Romano and M. Bellanger, "Fast least-squares adaptive notch filtering," *IEEE Trans. on Acoust., Speech, Signal Proc.*, vol. 36, June 1988.